Optimal control of the ballistic motion of Airy beams

Yi Hu,[1,2] Peng Zhang,[2] Cibo Lou,[1] Simon Huang,[2] Jingjun Xu,[1] and Zhigang Chen[1,2,*]

[1]*The Key Laboratory of Weak-Light Nonlinear Photonics, Ministry of Education and TEDA Applied Physics School, Nankai University, Tianjin 300457, China*

[2]*Department of Physics & Astronomy, San Francisco State University, San Francisco, California 94132, USA*

**Corresponding author: zhigang@sfsu.edu*

Received April 15, 2010; revised June 7, 2010; accepted June 8, 2010; posted June 16, 2010 (Doc. ID 127043); published June 29, 2010

We demonstrate the projectile motion of two-dimensional truncated Airy beams in a general ballistic trajectory with controllable range and height. We show that the peak beam intensity can be delivered to any desired location along the trajectory as well as repositioned to a given target after displacement due to propagation through disordered or turbulent media.

OCIS codes: 050.1970, 350.5500, 230.6120.

Airy beams have recently attracted a great deal of interest due to their unique properties [1–5] and potential applications in optical micromanipulation [6], plasma guidance [7], vacuum electron acceleration [8], and generation of three-dimensional optical bullets [9]. In practice, truncated Airy beams with finite energy have been established in laboratories, preserving the nondiffracting and self-accelerating properties over long distances. Such Airy beams can be generated linearly with a cubic phase mask [2–4], or during nonlinear processes [5,10]. In addition to Airy beams, other types of nondiffracting beams, such as accelerating parabolic beams, have also been demonstrated [11,12]. While, in most of the prior experiments, the path of a truncated accelerating beam follows simple projectile motion with the peak intensity fixed at the starting point, the natural question is how to make a beam propagate in a general ballistic trajectory and move its peak beam intensity to a given target along a controllable path.

In this Letter, we report our theoretical and experimental results on optimal control of the general ballistic trajectory of a truncated Airy beam. We show how a two-dimensional (2D) beam can be set into projectile motion, while the range and height of the trajectory can be controlled at ease without initial tilting of the input beam. Furthermore, the peak intensity of the Airy beam can be "delivered" to anywhere along the trajectory and can be repositioned to a given location after being displaced due to propagation through a disordered or turbulent medium. This brings about the possibility of sending an intense laser beam to a target while it passes through disordered media, such as turbulent fluids, and gets over obstacles.

We consider a typical optical system for generation of 2D Airy beams, as depicted in Fig. 1(a), where a Gaussian beam is first modulated by a cubic phase mask and then passes through a Fourier transform lens [2,3]. Usually, the Gaussian beam, the mask, and the Fourier lens are set to be coaxial along z. If the lens is transversely shifted, a tilting angle will be introduced into the Airy beam [3]. Here, we fix the position of the lens but allow the mask and Gaussian beam to have transverse displacements in the Fourier plane. To understand the influence of these displacements, let us first consider the one-dimensional case. The Fourier spectrum of a truncated Airy beam can be expressed as $\exp(-\alpha w^2)\exp[i(w^3-3\alpha^2 w-i\alpha^3)/3]$, where α is a small parameter for the exponential truncation factor, and w is the normalized wave number [1]. If the Gaussian beam and the phase mask are translated by w_g and w_m in the Fourier plane, the resulting spectrum $\exp[-\alpha(w-w_g)^2]\exp\{i[(w-w_m)^3-3\alpha^2(w-w_m)-i\alpha^3]/3\}$ leads to a new truncated Airy beam with a field envelope ϕ expressed as follows:

$$\phi = Cf(s,\xi)\mathrm{Ai}[s-w_m\xi-(\xi/2)^2 + i\alpha(\xi-2w_g+2w_m)]\exp(iw_m s), \tag{1a}$$

$$C = \exp(-\alpha {w_g}^2-\alpha {w_m}^2+i2\alpha^2 w_m-i2\alpha^2 w_g+2\alpha w_m w_g), \tag{1b}$$

$$f(s,\xi) = \exp[\alpha s+is\xi/2 + (-i{w_m}^2/2+i\alpha^2/2-2\alpha w_m+\alpha w_g)\xi + (-\alpha/2-iw_m/2)\xi^2-i\xi^3/12], \tag{1c}$$

where Ai represents the Airy function, and s and ξ are normalized transverse and longitudinal coordinates. From Eqs. (1), we see that the trajectory changes due to the translation of the mask as expressed by $s=w_m\xi+(\xi/2)^2$. The term $i\alpha(\xi-2w_g+2w_m)$ shows that the new peak-intensity position is at $\xi=2(w_g-w_m)$, controlled by translation of both the mask and the Gaussian beam. Applying similar analysis to the 2D case shown in Fig. 1(b), the trajectory can now be expressed as $-\sqrt{2}[D_m\xi/\sqrt{2}+(\xi/2)^2]$ with a new peak-intensity position at $\xi=-\sqrt{2}D_m+\sqrt{2}D_g$ (D_g and D_m are normalized vertical displacements of the Gaussian beam and the mask in the Fourier plane, respectively). Therefore, by translating the mask and Gaussian beam with respect to the z axis, the location of peak beam intensity, as well as maximum height and range of the trajectory, can be controlled with ease. Typical 2D numerical results are shown in Figs. 1(c) and 1(d). For $D_g=D_m=0$, the Airy beam propagates akin to a body projected horizontally, with the peak intensity appearing at the starting point. Moving the mask to different vertical positions ($D_m\approx -2.3,\ 3.1$) leads to propagation of the Airy beam in a ballistic trajectory, akin to a batted baseball. In the case of $D_g=0$, the peak intensity always appears at the maximum height. However, by

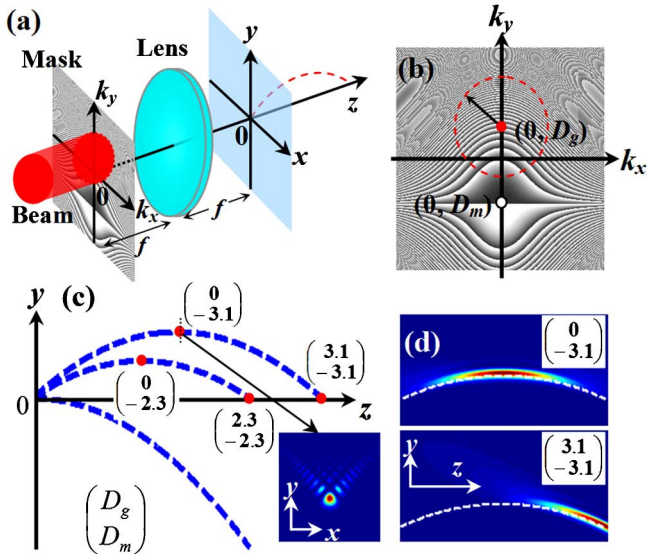

Fig. 1. (Color online) (a) Schematic of input Gaussian beam, cubic phase mask, and Fourier lens used for generation of truncated Airy beam. (b) Location of mask (center denoted by open circle) and input beam (marked by dashed circle and center denoted by solid dot) in the Fourier plane. (c) Illustration of different trajectories obtained at different D_g and D_m when the peak beam intensity appears at maximum heights or ranges (marked by dots). The inset shows the Airy beam profile at the maximum height of the upper curve. The lower curve corresponds to normal excitation at $D_g = D_m = 0$; so its peak intensity is at the starting point ($z = 0$). (d) Numerical simulations of beam propagation for two specific cases corresponding to the upper trajectory shown in (c).

translating also the Gaussian beam, so that $D_g = -D_m$, the peak intensity appears at the maximum range ("point of fall") as we shall demonstrate below.

In our experiment, a Gaussian beam ($\lambda = 632.8$ nm) is sent through a cubic phase mask assisted by a spatial light modulator (SLM) and then turned into a truncated Airy beam with a Fourier transform lens ($f = 150$ mm) [Fig. 1(a)]. A CCD camera is used to record the intensity pattern of the Airy beam at different propagation distances. To do so, the CCD camera is carefully repositioned along the z direction, and a reference Gaussian beam (without passing through the cubic mask) is used for calibration of the camera transverse position so that it has no lateral shift due to manual movement of the camera. When the beam, mask, and lens are aligned coaxially, a "horizontally projected" Airy beam is generated with a decaying intensity (due to diffraction) during propagation [Fig. 2(a)]. If only the mask is translated slightly in the vertical direction, the resulting Airy beam propagates in general ballistic trajectories with different ranges [Figs. 2(b) and 2(d)], while its peak intensity appears at the maximum heights. These different trajectories correspond to different launching angles due to the transverse displacement of the phase mask relative to the z axis of the system [3]. By translating the Gaussian beam the same distance, but to the opposite direction, the trajectory remains the same, but the peak intensity moves to the maximum range [Figs. 2(c) and 2(e)]. These experimental results agree well with our theoretical predictions.

If we allow both vertical and horizontal displacements of the phase mask $[(D_{mx}, D_{my})]$ and the Gaussian beam

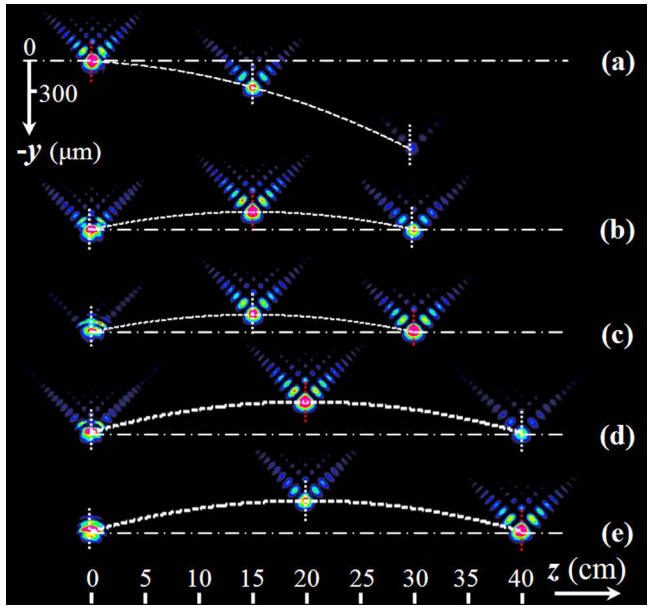

Fig. 2. (Color online) Experimental demonstration of controlled trajectories (dashed curves) of truncated Airy beams under different excitation conditions. Snapshots of transverse intensity patterns are shown at marked positions. (a) Normal condition when peak beam intensity is at the starting point, corresponding to lower curve in Fig. 1(c). (b), (d) Peak intensity goes to the maximum height with shifting of only the cubic phase mask. (c), (e) Peak intensity goes to the "point of fall" with additional shifting of the Gaussian beam.

$[(D_{gx}, D_{gy})]$, as illustrated in Fig. 3(a), the projectile motion of the Airy beam can be set into any arbitrary direction. Following similar theoretical analysis for Eqs. (1), the (x, y) trajectory can be expressed as $[-D_{mx}\xi, -D_{my}\xi - \sqrt{2}(\xi/2)^2]$. Clearly, the Airy beam in this case undergoes uniform motion along the horizontal direction while accelerating along vertical direction. As such, the Gaussian beam (even initially aiming along the z direction) can propagate to any off-axis location. The horizontal displacements of the mask and Gaussian beam will not change the location of the peak beam intensity, but they can change the Airy beam profile from symmetric (when $D_{mx} = D_{gx}$) to asymmetric (when $D_{mx} \neq D_{gx}$). Examples of the experimental results are shown in Figs. 3(b) and 3(c), where Fig. 3(b) is obtained by shifting only the mask along the diagonal direction ($D_{mx} = D_{my} = d < 0$; $d = -2.3$ in normalized units). The peak intensity appears at the maximum height of the trajectory when the Gaussian beam is on-axis [$D_{gx} = D_{gy} = 0$, shown in Fig. 3(b)], but it moves to the "point of fall" when the beam is displaced vertically [$D_{gx} = 0$, $D_{gy} = -d$, shown in Fig. 3(c)]. In this case, since $D_{mx} \neq D_{gx}$, the Airy beam starts with an asymmetric profile but evolves into a symmetric profile after restoring its peak intensity. These experimental observations are corroborated with numerical simulations.

The above control of an optical beam may find practical applications in transmission and reposition of the peak beam intensity to a target, even through disordered media. An example is illustrated in Fig. 4(a), where the peak intensity of a truncated Airy beam is supposed to land on a target located at $(x, y, z) = (0, 0, 25$ cm$)$ along a curved trajectory (dashed curve) after passing through a disordered medium. However, due to presence of the

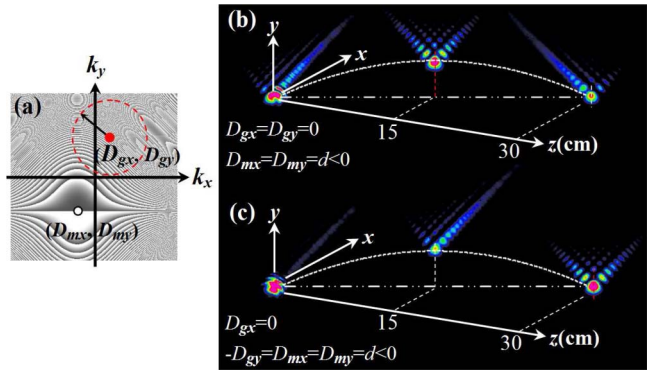

Fig. 3. (Color online) Experimental demonstration of accelerating Airy beams with transverse uniform motion. (a) Relative positions of cubic phase mask and Gaussian beam in the Fourier plane. (b), (c) Experimental results of the trajectory and intensity pattern of the Airy beam obtained under different excitation conditions as depicted in (a).

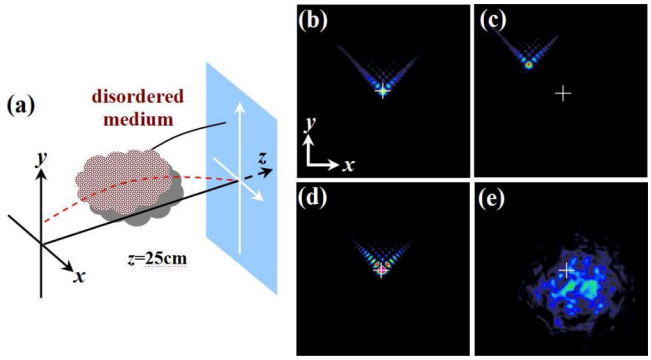

Fig. 4. (Color online) (a) Schematic of Airy beam propagation through a disordered medium. The dashed (solid) curve depicts the trajectory in free space (disordered medium). (b) Intensity pattern of output Airy beam at $z = 25$ cm through air and (c) stirred salt–water mixture. (d) Restoration of the Airy beam peak intensity at the target after translating the phase mask and input Gaussian beam. (e) Typical output pattern of a Gaussian beam from the salt–water mixture. The white cross corresponds to the target point at $(0, 0, 25$ cm$)$.

disordered medium, the Airy beam path (solid curve) is deflected off the target and diminishes in intensity during propagation. Simply by translating the phase mask and the initial Gaussian beam, the restored peak intensity can be repositioned at the target. Corresponding experimental results obtained with a turbulent salt–water mixture are shown in Figs. 4(b)–4(e). First, we "aim" the Airy beam at the target after 25 cm of propagation through air [Fig. 4(b)]. Then, salt is added and stirred in water placed in the beam path. Although the Airy beam is recovered through disordered scatters due to its self-healing property [4], its position in the target plane is shifted dramatically [Fig. 4(c)]. The large lateral shift of the Airy beam path from Figs. 4(b) and 4(c) is caused mainly by refraction from the salt–water mixture (which has a refractive index different from that of air), while small variation of the Airy beam in its shape and location in a given output plane occurs due to turbulence of the stirred mixture. By translating the mask and the Gaussian beam independently, as expected, not only does the Airy beam come back to the target, but its peak intensity is also restored [Fig. 4(d)]. We emphasize that Figs. 4(c) and 4(d) were taken as snapshots to show one example of the "fluctuating" pattern, as the shape and transverse position of the self-healing Airy beam vary slightly with time. However, the average intensity pattern is a well-defined Airy beam with its peak intensity repositioned at the target. For comparison, keeping all conditions the same as for Fig. 4(d), except for changing the cubic phase into uniform phase in the SLM, the Airy beam returns to a normal Gaussian beam that is severely scattered, deformed, and shifted after propagating through the same salt–water mixture [Fig. 4(e)]. These results suggest that Airy beams are excellent candidates for beam reposition to a given target through disordered or turbulent media, perhaps even with a feedback system that could compensate time-dependent fluctuation.

In summary, we have demonstrated optimal control of the ballistic motion of Airy beams. We have shown that the range and height of the beam trajectories can be controlled with ease, and the peak beam intensity can be delivered and repositioned to a given target after propagating through disordered or turbulent media. We mention that, by introducing the rotation of the cubic mask, the acceleration direction of the Airy beams can also be changed, representing an additional freedom for trajectory control. A similar method can be used for control of other accelerating beams, such as parabolic beams. Our results bring about possibilities for control of beam propagation and navigation in turbulent fluids.

This work was supported by the 973 Program (2007CB613203), the 111 Project, National Natural Science Foundation of China (NSFC), the Program for Changjiang Scholars and Innovative Research Team, the National Science Foundation (NSF), and the U.S. Air Force Office of Scientific Research (AFOSR).

References

1. G. A. Siviloglou and D. N. Christodoulides, Opt. Lett. **32**, 979 (2007).
2. G. A. Siviloglou, J. Broky, A. Dogariu, and D. N. Christodoulides, Phys. Rev. Lett. **99**, 213901 (2007).
3. G. A. Siviloglou, J. Broky, A. Dogariu, and D. N. Christodoulides, Opt. Lett. **33**, 207 (2008).
4. J. Broky, G. A. Siviloglou, A. Dogariu, and D. N. Christodoulides, Opt. Express **16**, 12880 (2008).
5. T. Ellenbogen, N. Voloch, A. Ganany-Padowicz, and A. Arie, Nat. Photon. **3**, 395 (2009).
6. J. Baumgartl, M. Mazilu, and K. Dholakia, Nat. Photon. **2**, 675 (2008).
7. P. Polynkin, M. Kolesik, J. V. Moloney, G. A. Siviloglou, and D. N. Christodoulides, Science **324**, 229 (2009).
8. J. Li, W. Zang, and J. Tian, Opt. Express **18**, 7300 (2010).
9. A. Chong, W. Renninger, D. N. Christodoulides, and F. W. Wise, Nat. Photon. **4**, 103 (2010).
10. I. Dolev, T. Ellenbogen, N. Voloch-Bloch, and A. Arie, Appl. Phys. Lett. **95**, 201112 (2009).
11. M. A. Bandres, Opt. Lett. **33**, 1678 (2008).
12. J. A. Davis, M. J. Mitry, M. A. Bandres, and D. M. Cottrell, Opt. Express **16**, 12866 (2008).